Acta Med. Okayama, 2012
Vol. 66, No. 2, pp. 143–154

Acta Medica Okayama
http://escholarship.lib.okayama-u.ac.jp/amo/

Original Article

Attenuated Sensory Deprivation-induced Changes of Parvalbumin Neuron Density in the Barrel Cortex of FcγRIIB-deficient Mice

Makiko Watanabe[a], Hiroshi Ueno[a], Shunsuke Suemitsu[b], Eriko Yokobayashi[c], Yosuke Matsumoto[d], Shinichi Usui[a], Hiroko Sujiura[a], and Motoi Okamoto[a]*

[a]*Department of Medical Technology, Graduate School of Health Sciences, Okayama University and* [d]*Department of Neuropsychiatry, Okayama University Graduate School of Medicine, Dentistry and Pharmaceutical Sciences, Okayama 700–8558, Japan,*
[b]*Koyodai Hospital, Maniwa, Okayama 719–3141, Japan,*
[c]*Department of Psychiatry, Kawasaki Medical University, Kurashiki, Okayama 701–0192, Japan*

Recent studies have demonstrated the important role of immune molecules in the development of neuronal circuitry and synaptic plasticity. We have detected the presence of FcγRIIB protein in parvalbumin-containing inhibitory interneurons (PV neurons). In the present study, we examined the appearance of PV neurons in the barrel cortex and the effect of sensory deprivation in FcγRIIB-deficient mice (FcγRIIB−/−) and wild-type mice. There was no substantial difference in the appearance of PV neurons in the developing barrel cortex between FcγRIIB−/− and wild-type mice. Sensory deprivation from immediately after birth (P0) or P7 to P12–P14 induced an increase in PV neurons. In contrast, sensory deprivation from P7 or P14 to P28, but not from P21 to P28, decreased PV neurons in wild-type mice. However, sensory deprivation from P0 or P7 to P12–P14 did not increase PV neurons and sensory deprivation from P7 or P14 to P28 did not decrease or only modestly decreased PV neurons in FcγRIIB−/− mice. The results indicate that expression of PV is regulated by sensory experience and the second and third postnatal weeks are a sensitive period for sensory deprivation, and suggest that FcγRIIB contributes to sensory experience-regulated expression of PV.

Key words: parvalbumin, fast-spiking interneurons, FcγRIIB, barrel cortex, sensory deprivation

Recent studies have demonstrated that molecules involved in immune function play important roles in the development of neuronal circuitry and synaptic plasticity [1–3]. The major histocompatibility complex class I (MHC I) is expressed in neurons [1, 2, 4–6]. Neurons with a deficit of β2-microglobulin (the noncovalently bound light chain of MHC I) or TAP1 (a transporter required to load peptides onto MHC l for delivery to the cell surface) fail to undergo normal activity-dependent refinement of the developing visual projection [6], and show higher synaptic density in the primary visual cortex [5]. Decreasing surface MHC I by transfection of siRNA increases glutamatergic and GABAergic synapse density in rat primary cultured cortical neurons [5]. A deficit of CD3ζ, the most common signal mediator of the MHC l receptor, disrupts the normal segregation of retinal afferents in the lateral geniculate nucleus [1, 3, 6]. Enhancement of long-term potentiation and the absence of long-term depression have been observed in the

Received September 6, 2011; accepted November 22, 2011.
*Corresponding author. Phone:+81–86–235–6883; Fax:+81–86–235–6883
E-mail:mokamoto@md.okayama-u.ac.jp (M. Okamoto)

hippocampi of CD3ζ-deficient mice [3, 6]. Among the receptors for the Fc portion of immunoglobulin G (FcγRs), FcγRl and FcγRlll couple with the gamma subunit. The gamma subunit is expressed in oligodendrocyte precursor cells, and deficiency of this subunit causes failure of normal myelination in the forebrain [7, 8]. FcγRllB is expressed in cerebellar Purkinje cells and Bergmann's glia, and a deficiency of FcγRllB results in abnormal synaptic connections between the parallel fibers and dendrites of Purkinje cells [9]. We have recently found that the FcγRllB protein is present in parvalbumin-containing interneurons (PV neurons) in the cerebral cortex of the mouse [10]. Because the FcγRllB protein is present in neonatal and adult PV neurons, we expected that FcγRllB might contribute to the maturation of PV neurons and plasticity of inhibitory synaptic connections.

PV neurons are a subpopulation of fast-spiking inhibitory interneurons and have been shown to appear in the neonatal period in the rodent cerebral cortex. Fast-spiking interneurons innervate the axon initial segment (axo-axonic or chandelier cells) or the cell bodies and proximal dendrites (basket or wide arbor cells) of principal neurons in the cerebral cortex and regulate action potential generation by principal neurons [11, 12]. In the barrel cortex, fast-spiking interneurons in the layer 4 receive direct thalamocortical inputs and exert strong feed-forward inhibition on spiny stellate cells [13, 14]contributing to an increase in the temporal resolutions of tactile information [13, 15]. Fast-spiking interneurons also contribute to receptive field sharpening [16, 17].

The appearance of PV neurons is coincident with the onset of a critical period for ocular dominance plasticity in the primary visual cortex [18]. The expression of PV is experience-dependent, and dark-rearing inhibits the expression of PV and retards the onset of the critical period for ocular dominance plasticity [18]. In the posterior medial portion of the rodent primary somatosensory cortex (barrel cortex), PV neurons appear around postnatal day 10 (P10) in layer 4 or layer 5 [19]. Sensory deprivation by whisker trimming for 3 weeks or 20 days from P7, but not from P15, retards the appearance of PV neurons [20, 21], but whisker plucking from P0 to P30 does not affect the number of PV neurons in layer 4 of the barrel cortex [22]. However, the precise chronological pattern in the appearance of PV neurons in each layer of the barrel cortex and the effects of short-term sensory deprivation on the expression of PV have not been fully examined [19, 21, 22].

In the present study, we examined the appearance of PV neurons in the developing barrel cortex and the effects of sensory deprivation on the appearance of PV neurons. Sensory deprivation from the first postnatal week to the end of the second postnatal week increased PV neurons, whereas sensory deprivation from postnatal day 7 (P7) or P14 to P28 decreased PV neurons in wild-type mice. In contrast, sensory deprivation from the first postnatal week to the end of the second postnatal week did not increase PV neurons and sensory deprivation from P7 or P14 to P28 did not decrease or only modestly decreased PV neurons in FcγRllB−/− mice. The results suggest that FcγRllB contributes to the experience-regulated expression of PV in fast-spiking interneurons.

Materials and Methods

Experimental animals. FcγRllB−/− mice were generated by homogeneous recombination as described previously [23]. The transgenic mice with a C57BL/6 × 129SvJ genetic background were backcrossed to C57BL/6N mice for 22 generations. FcγRllB+/+ littermates (wild-type) and FcγRllB−/− littermates were used in the present study. The day of birth was designated P0. Both male and female mice at P0, P7, P10, P12, P14, P16, P21, P28, and P56 were used.

This study was carried out in accordance with the National Institutes of Health (NIH) Guide for the Care and Use of Laboratory Animals (NIH Publications No. 80–23, revised in 1996) and approved by the Committee for Animal Experiments at Okayama University Advanced Research Center. All efforts were made to minimize the number of animals used and their suffering. The animals were housed in cages (4–8 animals per cage) with food and water provided ad libitum under 12-h light/dark conditions at 23–26℃.

Preparation of cryostat sections. The animals were anesthetized with diethyl ether (P21 and younger) or a lethal dose of sodium pentobarbital (Nembutal; Dainippon Sumitomo Pharma, Osaka, Japan; P28 and P56 animals, 100 mg/kg, i.p.) and transcardially perfused with ice-cold phosphate buffered saline (PBS) for 2 min, followed by 4% para-

formaldehyde and 0.2% picric acid in phosphate buffer, pH7.4, for 10 min. The brains were dissected and postfixed overnight in the same fixative at 4℃. They were then cryoprotected by incubation in 15% sucrose for 7 h followed by 30% sucrose for 20 h at 4℃. The brains were then frozen in O.C.T. Compound (Tissue-Tek; Sakura Finetek, Tokyo, Japan) by freezing in dry ice-cold normal hexane. Serial 25-μm coronal sections were prepared on a cryostat (CM-1900; Leica, Wetzlar, Germany) at −20℃. Sections at the barrel cortex level were collected in ice-cold PBS.

Cytochrome oxidase staining. The sections were washed in PBS and incubated in staining solution (1% sucrose, 0.05% nickel sulfate, 0.025% DAB, 0.015% cytochrome C, 0.01% catalase, 2.5 mM imidazole in 0.05 M phosphate buffer at pH7.4) for 2–3 h at 37℃. The sections were again washed in PBS, mounted on slides, and air-dried for 3 days. The slides were then washed in PBS, dehydrated and mounted.

Trypan blue staining. The cryostat sections were stained with 0.15% (w/v) trypan blue to identify the boundaries of layers and to verify the cytoarchitecture of the barrel cortex. To evaluate the thickness of the barrel cortex, we delineated its area, and the estimated area was divided by the length of the pial surface.

Immunohistochemical staining of PV neurons. The cryostat sections were washed in PBS, treated with 0.1% Triton X-100 in PBS (PBST) at room temperature for 15 min, washed again in PBS, and incubated in 0.3% H_2O_2 in PBST for 30 min. After 3 washes in PBS, the sections were incubated with 10% normal goat serum (Funakoshi Corporation, Tokyo, Japan) in PBS at room temperature for 1 h. After 3 washes in PBS, the sections were incubated with mouse anti-mouse PV antibody (clone PARV-19, P3088; Sigma-Aldrich Japan, Tokyo, Japan; 1 : 1000) in PBS overnight at 4℃. After being washed in PBS, the sections were incubated with biotin-conjugated rabbit anti-mouse IgG (MA01742-3049; Fitzgerald Industries International, Concord, MA, USA; 1 : 1000). After 3 washes in PBS, the sections were incubated with streptavidin-biotin-peroxidase conjugate (VECTASTAIN ABC kit; Vector Laboratories, Funakoshi Co.) for 1 h at room temperature. Immunoreactivity was visualized by incubating the samples in 50 mM Tris-HCl supplemented with 0.02% 2, 3-diaminobenzidine tetrahydrochloride (DAB, Sigma, St Louis, MO, USA), H_2O_2, and ammonium nickel sulfate hexahydrate.

Quantification of PV neurons. For preparation of digital images, light microscopic images (× 100) of the bilateral barrel cortices were captured by Lumina Vision software (version 2.4.0; Mitani Corporation, Fukui, Japan), and brightness and contrast were slightly adjusted. For quantification of PV neurons, immunohistochemical images captured by Lumina Vision software were analyzed using NIH ImageJ software (NIH, Bethesda, MD, USA; http://rsb.info.nih.gov/nih-image/). The quantification was performed by an observer who was blinded to the genotypes and sensory deprivation. Statistical comparisons were performed using Kruskal-Wallis H test or Mann-Whitney U test, and statistical significance was set at $p < 0.05$.

Double immunofluorescent labeling. The cryostat sections of P14 and P56 wild-type and FcγRIIB−/− mice were analyzed by double immunofluorescent staining of FcγRs and parvalbumin (PV). A rabbit polyclonal antibody against FcγRIIB (the generous gift of Masao Ono, Tohoku University, Sendai, Japan) or a rat anti-CD16/32 monoclonal antibody (clone 2.4G2; BD Biosciences, Tokyo, Japan) and a mouse monoclonal antibody against PV (PARV-19, Sigma-Aldrich Japan) were used for the detection of FcγRIIB or FcγRIII and PV, respectively. The sections were washed in PBS and treated with PBST at room temperature for 15 min. After 3 washes in PBS, the sections were incubated with 10% normal goat serum in PBS at room temperature for 1 h and then incubated with anti-FcγRIIB antibody (1 : 300) or anti-CD16/32 antibody (0.2 μg/ml) and anti-PV antibody (1 : 1000) in PBS overnight at 4℃. After being washed in PBS, the sections were incubated with rhodamine-conjugated anti-rabbit IgG (Molecular Probes, Millipore, Tokyo, Japan; 1 : 1000) or rhodamine-conjugated anti-rat IgG (BA-9400; Vector Laboratories Inc., Burlingame, CA, USA) and fluorescein isothiocyanate (FITC)-conjugated goat anti-mouse IgG (AP308F; Millipore, Tokyo, Japan; 1 : 100) in PBS at room temperature for 1 h. After 3 washes in PBS, the sections were mounted on glass slides with a ProLong Antifade Kit (P7481; Molecular Probes, Eugene, OR, USA) and covered

with cover slips.

Analysis of fluorescent images. The sections were observed under a confocal laser microscope (Zeiss 510; Carl Zeiss, Oberkochen, Germany) equipped with filters for rhodamine and FITC. Both 488- and 543-nm lasers lines were used for excitation, and 505- to 530-nm bandpass and 560-nm longpass filters were used for emission. Images were captured using the standard system operating software provided with the Zeiss 510 microscope (LSM Image Browser version 3.2).

Sensory deprivation (SD). To examine the effect of sensory deprivation (SD) on the appearance of PV neurons, all principal whiskers on the left snout were unilaterally trimmed to less than one mm in length from P0 to P12, P14, P21 or P28, or from P7, P14 or P21 to P28. Whisker trimming was also performed from P7 to P14. Animals were sacrificed at the end of SD under diethyl ether anesthesia or a lethal dose of sodium pentobarbital, and cryostat sections were stained with anti-PV antibody or anti-GAD67 antibody as described above. For evaluation of the effects of WT, quantification of PV neurons in the right barrel cortex (contralateral to the sensory deprived side) was performed as described above.

Results

FcγRIIB−/− mice grew normally and also behaved normally except that they sometimes neglected rearing. There was no difference in body weight, gross morphology or weight of the brain between FcγRIIB−/− mice and wild-type mice.

Localization of FcγRIIB protein. In the double immunofluorescent staining using antibodies against FcγRIIB and PV, FcγRIIB immunoreactivity was detected in PV neurons in the cerebral cortex of adult and neonatal wild-type mice, but not in those of FcγRIIB−/− mice (Fig. 1). FcγRIIB immunoreactivity was absent in microglial cells and astroglial cells. According to double immunofluorescent staining with anti-CD16/32 antibody and anti-PV antibody, CD16/32 immunoreactivity was detected in both microglial cells and PV neurons (data not shown).

Cytoarchitecture of the barrel cortex. It was easy to identify the barrel cortex because its thickness was greater than that of adjacent cerebral cortices at the level of the anterior half of the dorsal hippocampus. In addition, the barrels were confirmed by cytochrome oxidase staining of adjacent sections (data not shown). Trypan blue staining revealed a typical 6-layer organization of the barrel cortex both in wild-type and FcγRIIB−/− mice. There was no difference

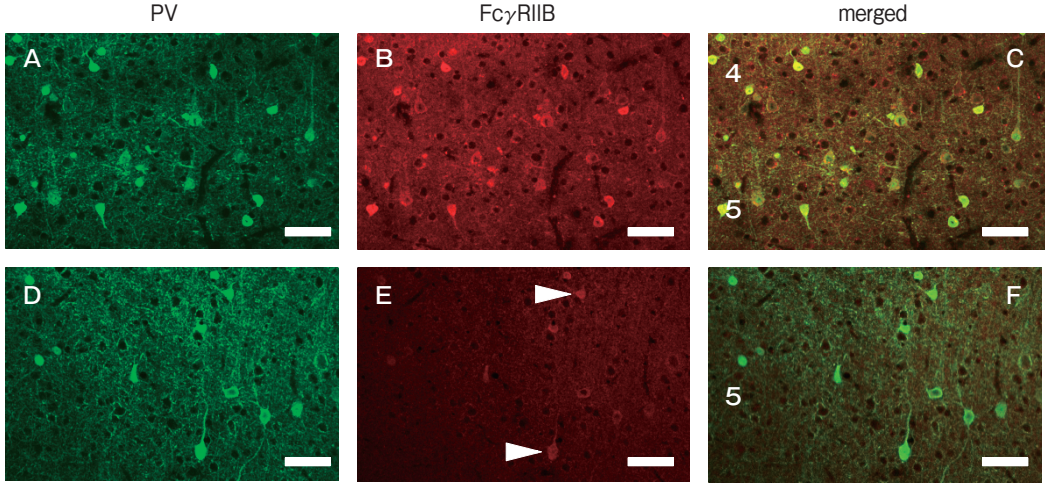

Fig. 1 Presence of the FcγRIIB protein in PV neurons. Confocal microscopic images of the barrel cortex of wild-type (**A**–**C**) and FcγRIIB−/− (**D**–**F**) mice at P14 are shown. The sections were stained with anti-FcγRIIB and anti-PV antibodies. Arabic numbers in the merged images indicate layers of the barrel cortex. The upper side is the pial surface. FcγRIIB fluorescence (red) overlaps with PV fluorescence (green) in the wild-type mice as evident in the merged image. No FcγRIIB-positive microglia are present. The faint FcγRIIB fluorescence (arrowheads) in the FcγRIIB−/− mice appeared to be a nonspecific staining. Scale bars: 50 μm.

in the light microscopic appearance and thickness of each layer of the barrel cortex between the wild-type and FcγRIIB−/− mice (data not shown). In cytochrome oxidase staining of tangential sections through layer 4, there was no difference in the size and arrangement of barrels between wild-type and FcγRIIB−/− mice at both P14 (Fig. 2) and P56 (data not shown).

Appearance of PV neurons in the barrel cortex. No PV-positive neuron was present in the barrel cortex at P7 either in wild-type or FcγRIIB−/− mice. A few PV neurons appeared in layers 4 at P10 (Fig. 3A and E). Many PV neurons were present in layers 4 and 5/6 at P12. These neurons had triangular or polygonal soma, and PV-positive mesh-like neurites appeared in the barrels of layer 4 (Fig. 3B and F). A few PV neurons were also present in layers 2/3. The number of PV neurons increased in layers 2/3 and 5/6 at P16 (Fig. 3C and G). The number of PV neurons further increased in layers 2/3 by P21. At the same time, mesh-like PV-positive neurites appeared in layers 2/3 and 5/6 (Fig. 3D and H).

There was no substantial difference in the appearance of PV neurons in the developing barrel cortex between wild-type and FcγRIIB−/− mice (Fig. 4). However, there were modest differences in the chronological pattern of the appearance of PV neurons between wild-type mice and FcγRIIB−/− mice when the density of PV neurons was measured in each layer of the barrel cortex. In layer 4, the density of PV neurons increased dramatically between P10 and P12 and reached a peak by P12 both in wild-type and FcγRIIB−/− mice (Fig. 4C). There was no difference in the PV neuron density between wild-type and FcγRIIB−/− mice except at P16, when the density of PV neurons was larger in FcγRIIB−/− mice than in wild-type mice (Fig. 4C). In layers 2/3, the density of PV neurons did not increase until P14, then increased between P14 and P21, and slightly decreased thereafter. In contrast, the density of PV neurons in FcγRIIB−/− mice was larger than that in wild-type mice at P14, but smaller than that in wild-type mice at P16 and P21 (Fig. 4B). In layers 5/6, the density of PV neurons increased between P10 and P16 (Fig. 4D). The density of PV neurons was larger in FcγRIIB−/− mice than in wild-type mice at P14 (Fig. 4D). The results indicate that the appearance of PV neurons differs depending on the layer of the barrel cortex, and that there is a critical period for the appearance of PV neurons in each layer of the barrel cortex (gray areas in Fig. 4B, C and D).

The effect of sensory deprivation (SD) on the appearance of PV neurons. We next examined the effect of SD on the appearance of PV neurons. All principal whiskers on the left snout were trimmed every day from P0 to P12, P14, P21 or P28. The effect of SD on the appearance of PV neurons was different between wild-type and FcγRIIB−/− mice. In wild-type mice, SD until P12 or P14, but not until P21 or P28, increased the number of PV neurons in the barrel cortex. SD from P0 to P12 increased the density of PV neurons by 25.6% and 43% in layers 4 and 5/6, respectively (Fig. 5C and D), but not in

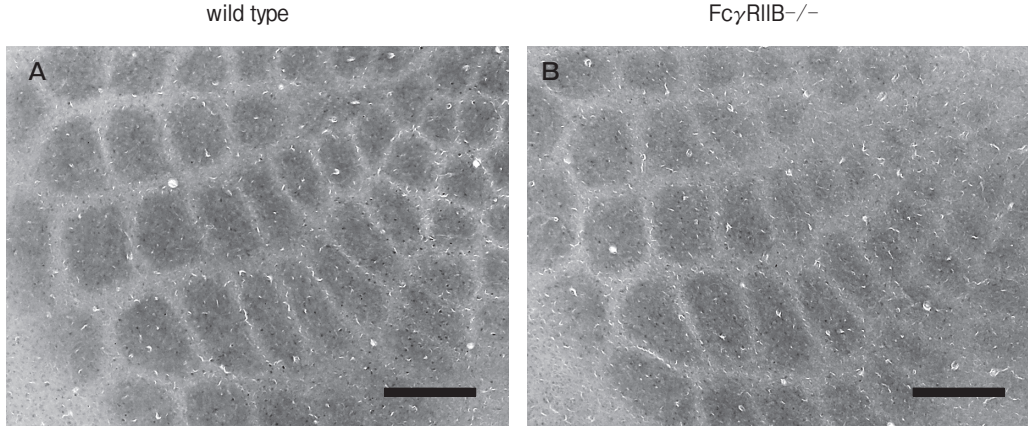

Fig. 2 Cytochrome oxidase staining. Tangential sections across layer 4 of the barrel cortex were stained by cytochrome oxidase staining. **A**, wild-type mouse at P14; **B**, FcγRIIB−/− mouse at P14. There was no difference in the arrangement and size of barrels between the wild-type mice and FcγRIIB−/− mice. Scale bars: 500 μm.

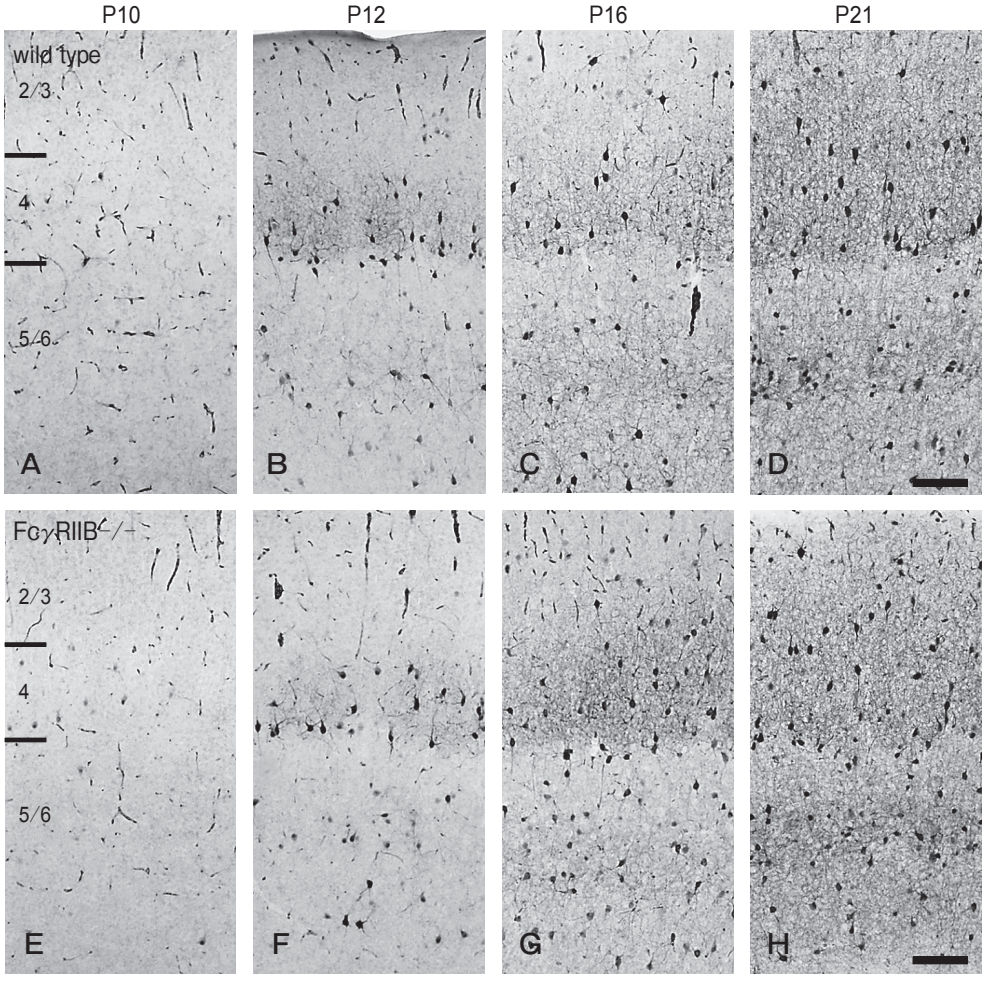

Fig. 3 Appearance of parvalbumin (PV) neurons in the barrel cortex. Sections of P10, P12, P16 and P21 animals stained with anti-PV antibody are shown. The upper (**A**–**D**) column shows the results for the barrel cortices of wild-type mice, and the lower column (**E**–**H**) shows the results for the barrel cortices of FcγRIIB−/− mice. Arabic numbers on the left side of **A** and **E** indicate layers of the barrel cortex. A few PV-positive cell bodies are present in layer 4 both in wild-type (**A**) and FcγRIIB−/− (**E**) mice at P10. Many triangular or polygonal PV-positive soma with PV-positive neurites are present in layers 2/3, 4, and 5/6 at P12 in both the wild-type (**B**) and Fc γ RIIB−/− (**F**) mice. In addition, mesh-like PV-positive neurites are present in layer 4. However, the number of PV neurons is smaller than that in P16 animals (**C** and **G**) in both layers 2/3 and 5/6. The number of PV neurons increased in layers 5/6 at P16. At P21, the number of PV neurons further increased in layers 2/3 and PV-positive mesh-like neurites appeared in layers 2/3 and 5/6. Scale bars: 100 μm.

layers 2/3 (Fig. 5B). SD from P0 to P14 increased the density of PV neurons by 175.6% and 29% in layers 2/3 and 5/6, respectively (Fig. 5B and D), but not in layer 4 (Fig. 5C). On the other hand, the density of PV neurons did not increase or even decreased when SD was continuously performed beyond P14. There was no difference in the density of PV neurons in layers 4 and 5/6 when SD was performed until P21 or P28 (Fig. 5C and D). In layers 2/3, the density of PV neurons decreased by 27% when SD was performed until P21 (Fig. 5B). Because PV neurons decrease by whisker trimming in the barrel cortex but the density of green fluorescent protein (GFP)-positive interneurons does not decrease in GFP-GAD67 transgenic mice [20], it is likely that the observed changes in the density of PV neurons by SD reflected the expression of PV rather than the proliferation or elimination of fast-spiking interneurons. Thus, the results suggest that SD by the end of the second postnatal week promotes the expression of

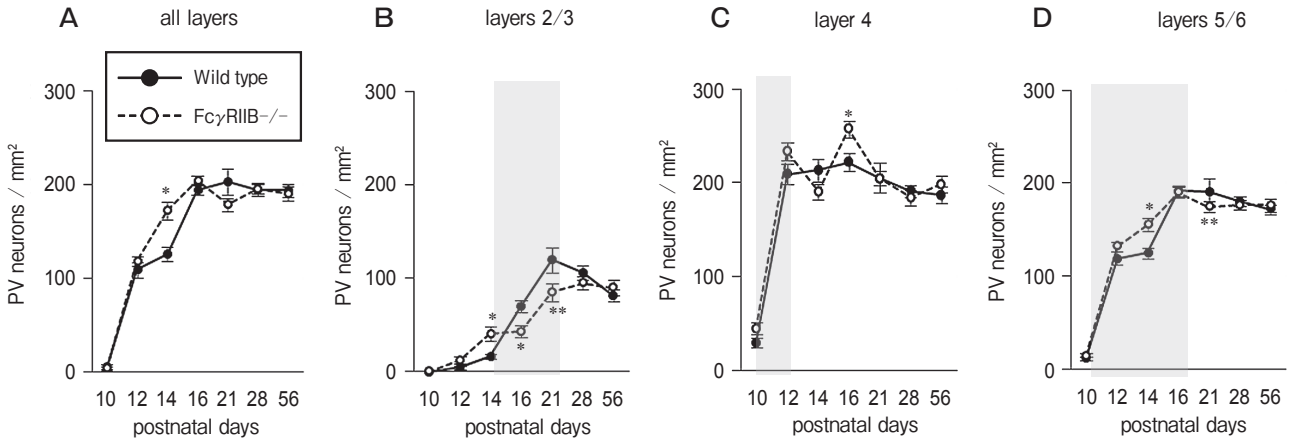

Fig. 4 Developmental changes in the density of PV neurons in the barrel cortex. The mean ± SEM values of the density of PV neurons per mm^2 in 12 to 20 sections from 3 to 6 animals are shown. There was no substantial difference in the developmental changes in the density of PV neurons between wild-type and FcγRIIB−/− mice when all layers were combined (**A**) except that the density of PV neurons was higher in FcγRIIB−/− mice compared to wild-type mice at P14. The developmental changes in the density of PV neurons differ depending on the layer of the barrel cortex. In layers 2/3 (**B**), the density of PV neurons did not increase by P14 in wild-type mice. It increased between P14 and P21, and slightly decreased thereafter. In contrast, the density of PV neurons increased between P12 and P14, but did not increase between P14 and P16 in FcγRIIB−/− mice. As a consequence, the density of PV neurons of FcγRIIB−/− mice was higher than that of wild-type mice at P14, but lower than that of wild-type mice at P16 and P21. In layer 4 (**C**), the density of PV neurons dramatically increased between P10 and P12 and reached a peak both in wild-type and FcγRIIB−/− mice. The density of PV neurons did not change thereafter, except that the density of PV neurons of FcγRIIB−/− mice was higher than that of wild-type mice at P16. In layers 5/6 (**D**), the density of PV neurons increased between P10 and P16. The density of PV neurons of FcγRIIB−/− mice was higher than that of wild-type mice at P14, but lower than that of wild-type mice at P21. $^*P < 0.05$, $^{**}P < 0.01$ by Mann-Whitney's U-test. Gray areas in **B**, **C** and **D** indicate the apparent critical period for the appearance of PV neurons.

PV, whereas SD extended beyond the third postnatal week inhibits or does not affect the expression of PV.

In contrast, SD did not increase the density of PV neurons in FcγRIIB−/− mice (Fig. 5). In contrast to the increase of PV neuron density in wild-type mice, SD from P0 to P14 decreased the density of PV neurons by 23% in layers 5/6 (Fig. 5D), and SD from P0 to P28 decreased the density of PV neurons by 14% in layer 4 (Fig. 5C). The results indicate that PV neurons of FcγRIIB−/− mice are relatively insensitive to SD compared to wild-type mice, and SD by the end of the second postnatal week does not promote the expression of PV in FcγRIIB−/− mice.

The increase of PV neurons by SD by the end of the second postnatal week may have been due to the whisker trimming begun before the critical period for the formation of barrels in layer 4. To confirm this point, we trimmed all principal whiskers on the left snout from P7 to P14, because the barrels in layer 4 are formed by P5. When the principal whiskers were trimmed from P7 to P14, the densities of PV neurons in layers 2/3 and 5/6 were 3.95-fold and 1.32-fold higher than those in intact wild-type mice, but the density in layer 4 was 14% lower than that in intact wild-type mice (Fig. 6). The results were similar to those for wild-type mice deprived from P0 to P14 (Fig. 5). In FcγRIIB−/− mice, SD from P7 to P14 increased the density of PV neurons by 1.52 fold compared to that in intact mice in layers 2/3 (Fig. 6), but the increase was not significant (mean ± SEM: intact mice, 40.9 ± 7.3 in 20 sections; deprived mice, 62.2 ± 7.9 in 14 sections; $p = 0.057$). SD from P7 to P14 decreased the density of PV neurons by 14% in layers 5/6 in FcγRIIB−/− mice, while the same treatment increased the PV neurons in these layers in wild-type mice (Fig. 6). SD from P7 to P14 decreased the density of PV neurons by 16% in layer 4 as in wild-type mice (Fig. 6). Thus, SD from P7 to P14 increased the PV neuron density as in animals who were subjected to SD from P0 to P14 in layers 2/3 and 5/6 of wild-type mice, but decreased the PV neuron density in layers 5/6 of FcγRIIB−/− mice. However, SD from P7 to P14 increased the PV neuron density in layers 2/3 of FcγRIIB−/− mice in

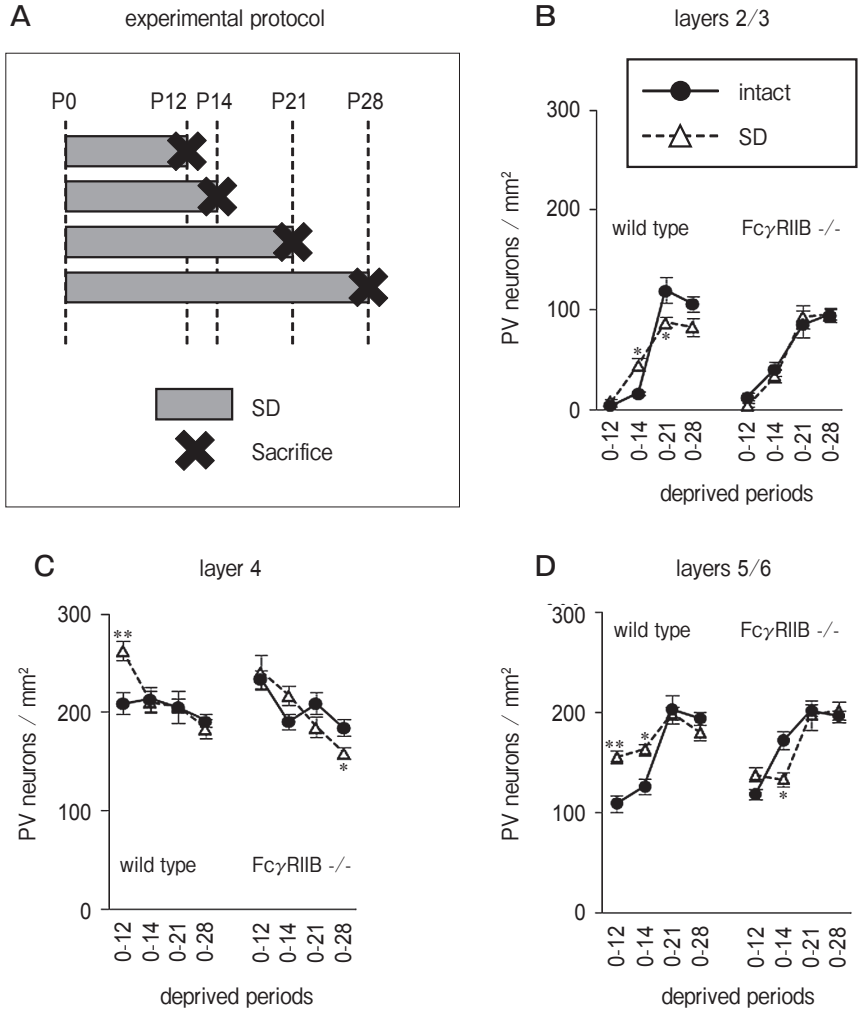

Fig. 5 The effect of sensory deprivation (SD) from P0 on the density of PV neurons in each layer of the barrel cortex. The mean ± SEM values of the density of PV neurons per mm^2 in 6 to 30 sections from 3 to 6 animals are shown. All principal whiskers on the left snout were trimmed every day from P0 to P12, P14, P21 or P28 as shown in **A**. Closed circles represent the values of intact mice and open triangles represent the values of trimmed mice. The results in wild-type mice are shown on the left side and the results in FcγRIIB−/− mice are shown on the right side in **B**, **C** and **D**. **B**, layers 2/3. SD until P12 had no effect on the number of PV neurons, probably because PV neurons did not appear at P12. SD until P14 significantly increased the density of PV neurons, while SD until P21 significantly decreased the density of PV neurons in wild-type mice. In contrast, SD did not cause a change in the density of PV neurons in FcγRIIB−/− mice; **C**, layer 4. SD until P12 significantly increased the density of PV neurons, while SD until P14, P21 and P28 did not cause changes in the density of PV neurons in wild-type mice. In FcγRIIB−/− mice, in contrast, SD until P12, P14 and P21 did not cause significant change in the density of PV neurons, while SD until P28 significantly decreased the density of PV neurons; **D**, layers 5/6. SD until P12 and P14 significantly increased the density of PV neurons while SD until P21 and P28 had no effect on the density of PV neurons in wild-type mice. In FcγRIIB−/− mice, SD until P12, P21 and P28 did not cause change in the density of PV neurons, while SD from P0 to P14 significantly decreased the density of PV neurons. $^{*}P < 0.05$, $^{**}P < 0.01$ compared to intact animals by Mann-Whitney's U-test. SD, sensory deprivation.

contrast to the results for FcγRIIB−/− mice subjected to SD from P0 to P14. In layer 4, SD from P7 to P14 decreased the PV neuron density both in wild-type and FcγRIIB−/− mice, although SD from P0 to P14 did not decrease the PV neuron density either in wild-type or FcγRIIB−/− mice. The results indicate that the increase of PV neuron density in layers 2/3 and 5/6 of wild-type mice was not due to whisker

trimming begun before the formation of barrels, and suggest that the effect of sensory deprivation on the PV neuron density in layer 4 differs according to whether SD is begun before or after the critical period for the formation of barrels.

These results suggest the presence of a restricted developmental time window when expression of PV is sensitive to SD. To further explore this point we compared the effects of SD from P0, P7, P14 or P21 to P28 on the appearance of PV neurons. SD from P7 or P14, but not from P0 or P21, significantly decreased the density of PV neurons in layers 4 and 5/6 in wild-type mice (Fig. 7C and D). The densities of PV neurons in layer 4 of wild-type mice deprived from P7 to P28 and from P14 to P28 were 81.7% and 85.6% of those in intact wild-type mice at P28, respectively (Fig. 7C). The reduction of PV neurons in layer 4 by SD from P7 to P28 was consistent with the previous study [20]. The densities of PV neurons in layers 5/6 of wild-type mice deprived from P7 to P28 and from P14 to P28 were 78.9% and 76.7% of those in intact wild-type mice at P28, respectively (Fig. 7D). PV neurons were also decreased by SD in layers 2/3, but the difference was not significant (Fig. 7B). The effects of SD in FcγRIIB−/− mice were different from those in wild-type mice. SD did not cause a change of the PV neuron density in layers 2/3 in FcγRIIB−/− mice (Fig. 7B). SD from P0 to P28 significantly decreased the PV neuron density in layer 4, as described above (see Fig. 5C), but SD from P7, P14 or P21 did not cause a change of the PV neuron density (Fig. 7C). The densities of PV neurons in layers 5/6 of FcγRIIB−/− mice deprived from P14 to P28 and from P21 to P28 were 89% and 90% of those in intact FcγRIIB−/− mice at P28, respectively (Fig. 7D). SD from P0 or P7 to P28 did not decrease the PV neuron density in FcγRIIB−/− mice (Fig. 7D). The results suggest that the expression of PV is reduced by SD throughout the second and third postnatal weeks in wild-type mice, and that PV neurons of FcγRIIB−/− mice are relatively insensitive to SD.

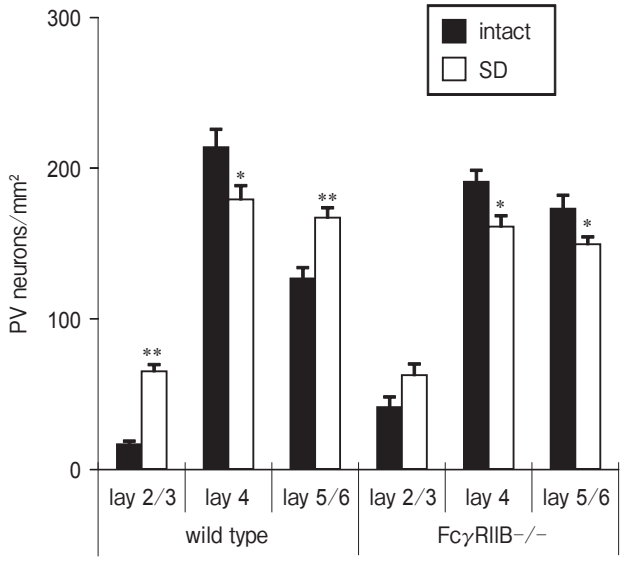

Fig. 6 The effect of sensory deprivation (SD) from P7 to P14 on the density of PV neurons in each layer of the barrel cortex. The mean ± SEM values of the density of PV neurons per mm² in 15 (wild-type mice) or 14 (FcγRIIB−/− mice) sections from 4 animals are shown. All principal whiskers on the left snout were trimmed every day from P7 to P14. Closed bars represent the values of intact mice and open bars represent the values of mice that underwent whisker-trimming. SD significantly increased the density of PV neurons in layers 2/3 and 5/6, while it significantly decreased the density of PV neurons in layer 4 in wild-type mice. In FcγRIIB−/− mice, SD did not significantly increase the density of PV neurons in layers 2/3 but significantly decreased the density of PV neurons in layers 5/6. On the other hand, SD significantly decreased the density of PV neurons in layer 4 as in wild-type mice. $^{*}P < 0.05$, $^{**}P < 0.01$ compared to intact mice by Mann-Whitney's U-test. SD, sensory deprivation.

Discussion

In the present study we demonstrated the appearance of PV neurons in the developing barrel cortex and the effect of sensory deprivation on the appearance of PV neurons in wild-type and FcγRIIB−/− mice.

There were slight differences in the appearance of PV neurons in the developing barrel cortex between wild-type and FcγRIIB−/− mice. The number of PV neurons in the developing barrel cortex dramatically changed depending on the duration after birth, as shown in Fig. 4. A difference of only one-half or one day had prominent influences on the number of PV neurons. Therefore, it is likely that there is no essential difference in the appearance of PV neurons in the developing barrel cortex between wild-type and FcγRIIB−/− mice. An exception is that the density of PV neurons of FcγRIIB−/− mice was higher than that in wild-type mice at P14, whereas it was lower than that in wild-type mice at P16 and P21 in layers 2/3 (Fig. 4B).

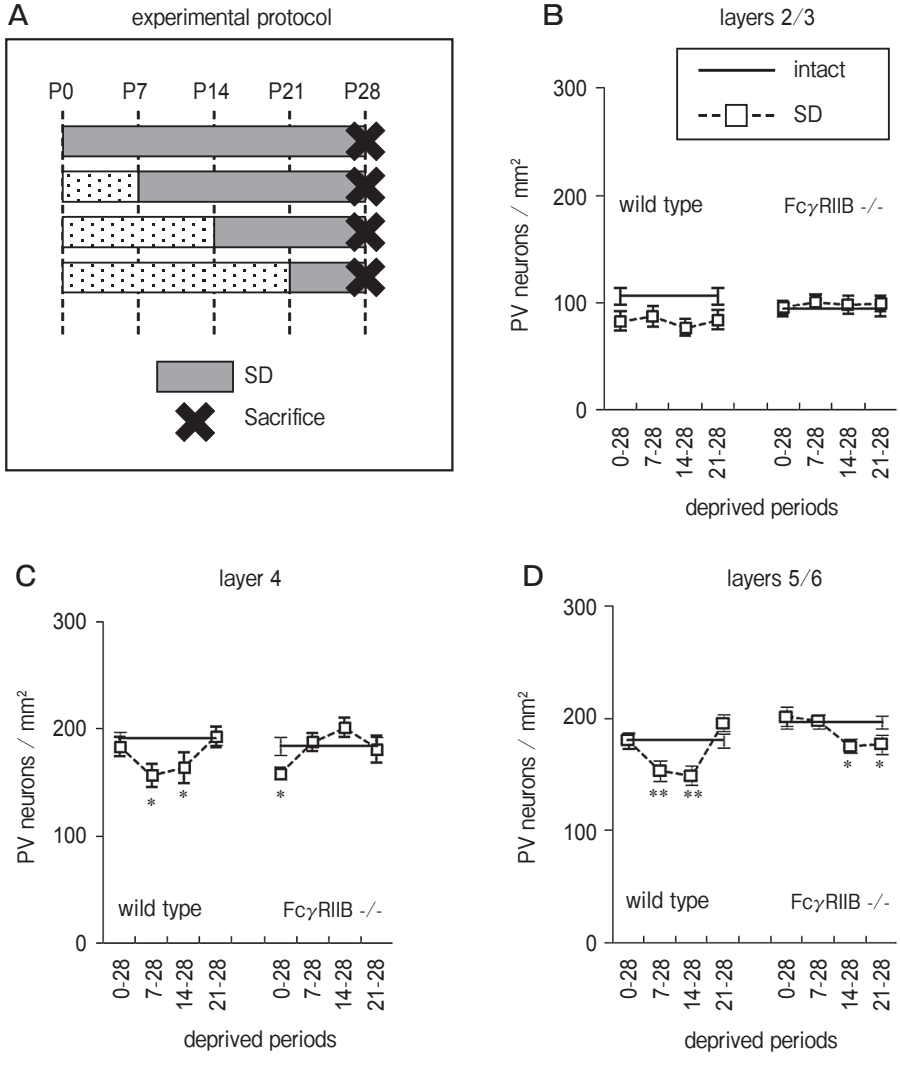

Fig. 7 The effect of sensory deprivation (SD) from P0, P7, P14 and P21 to P28 on the density of PV neurons in each layer of the barrel cortex. The mean ± SEM values of the density of PV neurons per mm^2 in 9 to 15 sections from 3 to 6 animals are shown. All principal whiskers on the left snout were trimmed every day from P0, P7, P14 or P21 to P28 as shown in **A**. The horizontal bars represent the values of intact mice at P28. Open squares represent the values of mice undergoing whisker trimming. The results in wild-type mice are shown on the left side and the results in FcγRIIB−/− mice are shown on the right side in **B**, **C** and **D**. **B**, layers 2/3. The density of PV neurons was decreased by SD in wild-type mice, but the difference was not significant. SD did not affect the density of PV neurons in FcγRIIB−/− mice; **C**, layer 4. SD from P7 and P14 to P28 significantly decreased the density of PV neurons in wild-type mice. In FcγRIIB−/− mice, the density of PV neurons was significantly decreased by SD from P0 to P28, but not SD from P7, P14 and P21 to P28; **D**, layers 5/6. SD from P7 and P14 to P28 significantly decreased the density of PV neurons in wild-type mice. In FcγRIIB−/− mice, the density of PV neurons was only modestly decreased by SD from P14 and P21 to P28, but not by SD from P0 and P7 to P28. $^{*}P < 0.05$, $^{**}P < 0.01$ compared to intact mice by Mann-Whitney's U-test SD, sensory deprivation.

The most interesting finding in our study was that PV neuron density was increased in sensory deprived wild-type mice but was not increased in sensory deprived FcγRIIB−/− mice. The density of PV neurons in wild-type mice subjected to sensory deprivation from P0 was significantly higher than that in intact wild-type mice at P12 and/or P14. The density of PV neurons in FcγRIIB−/− mice subjected to sensory deprivation from P0 was similar to that in intact FcγRIIB−/− mice at P12 and P14, except in layers 5/6 at

P14 (Fig. 5). The increase of PV neurons by sensory deprivation was likely the result of an increase of PV expression rather than the proliferation of fast-spiking interneurons. An increase of PV neurons in the cerebral cortex by sensory deprivation has not been reported. Sensory deprivation from P0 to P12, but not deprivation from P0 or P7 to P14, increased PV neurons in layer 4 of wild-type mice (Fig. 5C). Sensory deprivation from P0 to P14, but not deprivation from P0 to P12, increased PV neurons in layers 2/3 (Fig. 5B). The mechanism underlying the increase of PV expression is not clear. In layer 4, excitatory postsynaptic currents (EPSCs) in fast-spiking interneurons induced by stimulation of thalamocortical afferent has been shown to dramatically increase by P9–11 [13]. In fast-spiking interneurons of layers 2/3, the amplitude of EPSCs significantly increases after P15 [16]. The maturation of EPSCs depends, at least in part, on the substitution of the NMDA receptor subunit from NR2B to NR2A. Selective blocking of NR2A from P7 to P17 retards the appearance of PV neurons in layers 2/3 and 4 [16]. Substitution of the NMDA receptor subunit from NR2B to NR2A occurs at P12–14 in layers 2/3 [16]. On the other hand, selective axonal projection from layer 4 spiny stellate cells to layer 2/3 neurons in the same sensory column is established by P14 [24]. Sensory deprivation does not affect the development of axonal projection from spiny stellate cells to layer 2/3 neurons [24]. Thus the maturation of electrophysiological properties and subunit composition of NMDA receptors in PV neurons occurs around P10 in layer 4 and at P12–P14 in layers 2/3. The number of PV neurons dramatically increases after P10 in layer 4 and after P14 in layers 5/6. Therefore it is clear that the maturation of NMDA receptors is required for the expression of PV in fast-spiking interneurons, although it remains uncertain whether this is also the case in layers 5/6, because the development of excitatory input to fast-spiking interneurons in layers 5/6 has not been examined. Therefore, sensory deprivation begun at a time point just around the maturation of NMDA receptors in fast-spiking interneurons may upregulate the expression of PV. Importantly, the increase of PV neurons by sensory deprivation was not observed in FcγRIIB−/− mice, whereas the appearance of PV neurons in intact FcγRIIB−/− mice was similar to that in wild-type mice. Together, these results suggest that PV neurons of FcγRIIB−/− mice are relatively insensitive to sensory deprivation and FcγRIIB is involved in the upregulation of PV expression induced by sensory deprivation.

The PV neuron density was decreased by sensory deprivation from P7 or P14 to P28 in layers 4 and 5/6 of wild-type mice. The density of PV neurons did not decrease by deprivation from P0 or P21 to P28. The results suggest that there is a sensitive time window when sensory deprivation downregulates the expression of PV, and that continuous sensory deprivation beyond the maturation of NMDA receptors in fast-spiking interneurons downregulates the expression of PV. The decrease of PV neuron density by sensory deprivation from P7 to P28 is consistent with the previous study [20]. However, the reduction of PV neuron density in layer 4 by sensory deprivation from P14 to P28 is inconsistent with the absence of the reduction of PV neurons in mice subjected to sensory deprivation from P15 to P30 in the previous study [20]. The reason for this discrepancy is not clear. In the GFP-GAD67 transgenic mice used in the previous study, whisker trimming caused atrophy of barrels corresponding to the trimmed row, whereas whisker trimming after P7 does not usually cause atrophy of barrels [17]. This discrepancy between our study and the previous study [17] may have been at least partly due to the difference in the genetic background. Again, the effects of sensory deprivation on the expression of PV in FcγRIIB−/− were different from those in wild-type mice. Sensory deprivation from P7 to P28 did not cause a change in the density of PV neurons. Sensory deprivation from P14 or P21 to P28 slightly decreased the PV neuron density in layers 5/6, but not in layers 2/3 and 4 (Fig. 7). The results indicate that PV neurons of FcγRIIB−/− mice are relatively insensitive to sensory deprivation after the maturation of NMDA receptors and suggest that FcγRIIB may also contribute to the downregulation of PV expression by sensory deprivation.

The expression of PV and maturation of inhibitory neuronal circuitry is sensitive to sensory experience [13]. The results of the present study show that the change of PV expression induced by sensory deprivation is absent or attenuated in FcγRIIB−/− mice. Interestingly, the density of PV neurons in layers 2/3 of FcγRIIB−/− mice was higher than that in wild-type mice at P14, whereas it was lower than that in wild-

type mice at P16 and P21 (Fig. 4B). This developmental profile of the density of PV neurons in layers 2/3 of FcγRIIB−/− mice is quite similar to that in layers 2/3 of sensory deprived wild-type mice (Fig. 5B). Together, these results suggest that the response of PV neurons to excitatory inputs from spiny stellate cells is impaired in FcγRIIB−/− mice, and that FcγRIIB contributes to the experience-regulated expression of PV, although further studies are required to clarify the mechanism underlying the altered response of PV neurons to sensory deprivation.

References

1. Boulanger LM: Immune proteins in brain development and synaptic plasticity. Neuron (2009) 64: 93–109.
2. Boulanger LM and Shatz CJ: Immune signaling in neural development, synaptic plasticity and disease. Nat Rev Neurosci (2004) 5: 521–531.
3. Boulanger LM, Huh GS and Shatz CJ: Neuronal plasticity and cellular immunity: shared molecular mechanisms. Curr Opin Neurobiol (2001) 11: 568–578.
4. Corriveau RA, Huh GS and Shatz CJ: Regulation of class I MHC gene expression in the developing and mature CNS by neural activity. Neuron (1998) 21: 505–520.
5. Glynn MW, Elmer BM, Garay PA, Liu XB, Needleman LA, El-Sabeawy F and McAllister AK: MHCI negatively regulates synapse density during the establishment of cortical connections. Nat Neurosci (2011) 14: 442–451.
6. Huh GS, Boulanger LM, Du H, Riquelme PA, Brotz TM and Shatz CJ: Functional requirement for class I MHC in CNS development and plasticity. Science (2000) 290: 2155–2159.
7. Nakahara J, Seiwa C, Shibuya A, Aiso S and Asou H: Expression of Fc receptor for immunoglobulin M in oligodendrocytes and myelin of mouse central nervous system. Neurosci Lett (2003) 337: 73–76.
8. Nakahara J, Tan-Takeuchi K, Seiwa C, Gotoh M, Kaifu T, Ujike M, Yagi T, Ogawa M, Takai T, Aiso S and Asou H: Signaling via immunoglobulin Fc receptors induces oligodendrocyte precursor cell differentiation. Dev Cell (2003) 4: 841–852.
9. Nakamura K, Hirai H, Torashima T, Miyazaki T, Tsurui H, Xiu Y, Ohtsuji M, Lin QS, Tsukamoto K, Nishimura H, Ono M, Watanabe M and Hirose S: CD3 and immunoglobulin G Fc receptor regulate cerebellar functions. Mol Cell Biol (2007) 27: 5128–5134.
10. Suemitsu S, Watanabe M, Yokobayashi E, Usui S, Ishikawa T, Matsumoto Y, Yamada N, Okamoto M and Kuroda S: Fc gamma receptors contribute to pyramidal cell death in the mouse hippocampus following local kainic acid injection. Neuroscience (2010) 102: 2955–2973.
11. Huang ZJ, Di Cristo G and Ango F: Development of GABA innervation in the cerebral and cerebellar cortices. Nat Rev Neurosci (2007) 8: 673–686.
12. Lewis DA, Hashimoto T and Volk DW: Cortical inhibitory neurons and schizophrenia. Nat Rev Neurosci (2005) 6: 312–324.
13. Chittajallu R and Isaac JT: Emergence of cortical inhibition by coordinated sensory-driven plasticity at distinct synaptic loci. Nat Neurosci (2010) 13: 1240–1248.
14. Sun QQ, Huguenard JR and Prince DA: Barrel cortex microcircuits: thalamocortical feedforward inhibition in spiny stellate cells is mediated by a small number of fast-spiking interneurons. J Neurosci (2006) 26: 1219–1230.
15. Gabernet L, Jadhav SP, Feldman DE, Carandini M and Scanziani M: Somatosensory integration controlled by dynamic thalamocortical feed-forward inhibition. Neuron (2005) 48: 315–327.
16. Zhang Z and Sun QQ: Development of NMDA NR2 subunits and their roles in critical period maturation of neocortical GABAergic interneurons. Dev Neurobiol (2011) 71: 221–245.
17. Foeller E and Feldman DE: Synaptic basis for developmental plasticity in somatosensory cortex. Curr Opin Neurobiol (2004) 14: 89–95.
18. Tropea D, Kreiman G, Lyckman A, Mukherjee S, Yu H, Horng S and Sur M: Gene expression changes and molecular pathways mediating activity-dependent plasticity in visual cortex. Nat Neurosci (2006) 9: 660–668.
19. Itami C, Kimura F and Nakamura S: Brain-derived neurotrophic factor regulates the maturation of layer 4 fast-spiking cells after the second postnatal week in the developing barrel cortex. J Neurosci (2007) 27: 2241–2252.
20. Jiao Y, Zhang C, Yanagawa Y and Sun QQ: Majoe effects of sensory experience on the neocortical inhibitory circuits. J Neurosci (2006) 26: 8691–8701.
21. Sun QQ: Experience-dependent intrinsic plasticity in interneurons of barrel cortex layer IV. J Neurophysiol. (2009) 102: 2955–2973.
22. McRae PA, Rocco MM, Kelly G, Brumberg JC and Matthews RT: Sensory deprivation alters aggrecan and perineuronal net expression in the mouse barrel cortex. J Neurosci (2007) 27: 5405–5413.
23. Takai T, Ono M, Hideki M, Ohmori H and Ravetch JV: Augmented humoral and anaphylactic responses in Fc gamma RII-deficient mice. Nature (1996) 379: 346–349.
24. Bender KJ, Rangel J and Feldman DE: Development of columnar topography in the excitatory layer 4 to layer 2/3 projection in rat barrel cortex. J Neurosci (2003) 23: 8759–8770.